

Strong and Electroweak Corrections to the Production of a Higgs Boson + 2 Jets via Weak Interactions at the Large Hadron Collider

M. Ciccolini,¹ A. Denner,¹ and S. Dittmaier²

¹Paul Scherrer Institut, Würenlingen und Villigen, CH-5232 Villigen PSI, Switzerland

²Max-Planck-Institut für Physik (Werner-Heisenberg-Institut), D-80805 München, Germany

(Received 4 July 2007; published 19 October 2007)

Radiative corrections of strong and electroweak interactions are presented at next-to-leading order for the production of a Higgs boson plus two hard jets via weak interactions at the CERN Large Hadron Collider. The calculation includes all weak-boson fusion and quark-antiquark annihilation diagrams as well as the corresponding interferences. The electroweak corrections, which are discussed here for the first time, reduce the cross sections by 5% and thus are of the same order of magnitude as the QCD corrections.

DOI: [10.1103/PhysRevLett.99.161803](https://doi.org/10.1103/PhysRevLett.99.161803)

PACS numbers: 12.15.Lk, 13.40.Ks, 13.85.Qk, 14.80.Bn

Introduction.—The production of a standard Higgs boson in association with two hard jets is a cornerstone in the Higgs boson search both in the ATLAS [1] and compact muon solenoid [2] experiments at the LHC for the Higgs boson mass range between 100 and 200 GeV, which is favored by the global standard model fit to electroweak (EW) precision data [3].

The production of a Higgs boson + 2 jets receives two kinds of contributions at hadron colliders. The first type, where the Higgs boson couples to a weak boson that links two quark lines, is dominated by squared t - and u -channel-like diagrams and known as the “vector-boson fusion” (VBF) channel. The hard jet pairs have a strong tendency to be forward-backward directed in contrast to other jet production mechanisms, offering a good background suppression (transverse momentum and rapidity cuts on jets, jet rapidity gap, central-jet veto, etc.). Upon applying appropriate event selection criteria (see, e.g., Refs. [4–10] for more references) it is possible to sufficiently suppress background and to enhance the VBF channel over the second $H + 2$ jets mechanism that mainly proceeds via strong interactions. In this second channel the Higgs boson is radiated off a heavy-quark loop that couples to any parton of the incoming hadrons via gluons [11,12]. According to a recent estimate [13] hadronic production contributes about 4–5% to the Higgs boson + 2 jets events for a Higgs boson mass of 120 GeV after applying VBF cuts. A next-to-leading order (NLO) analysis [12] of this contribution shows that its residual scale dependence is still of the order of 35%.

Higgs boson production in the VBF channel is a pure EW process in leading order (LO) involving only quark and antiquark parton distributions. Approximating the cross section by t - and u -channel diagrams only (without interference), because s -channel diagrams and interferences are rather suppressed, the corresponding NLO QCD corrections reduce to vertex corrections to the weak-boson-quark coupling. Explicit NLO QCD calculations in this approximation [10,14–17] confirm the expectation that these QCD corrections are quite small, because

they are shifted to the parton distribution functions (PDF) via QCD factorization to a large extent. The resulting QCD corrections are of the order of 5–10% and reduce the remaining factorization and renormalization scale dependence of the NLO cross section to a few percent.

In this Letter we complete the previous NLO calculations for the VBF channel in two respects. Firstly, we add the complete NLO EW corrections, and secondly we include all interferences in the QCD corrections. While all interferences are negligibly small, as expected, the EW corrections are of the same size as the QCD corrections and thus phenomenologically relevant. For a full simulation of the production of Higgs boson + 2 jets at the LHC, the contribution of the gluon-induced channel has to be added to our results. Since the Higgs boson is treated as a stable particle, which is a good approximation up to intermediate Higgs boson masses, the generated events eventually have to be interfaced to dedicated Higgs boson decay generators in the full simulation.

Details of the NLO calculation.—At LO, the production of Higgs boson + 2 jets via weak bosons receives contributions from the partonic processes $qq \rightarrow Hqq$, $q\bar{q} \rightarrow Hq\bar{q}$, $\bar{q}\bar{q} \rightarrow H\bar{q}\bar{q}$. For each relevant configuration of external quark flavors one or two of the topologies shown in Fig. 1 contribute. All LO and one-loop NLO diagrams are related by crossing symmetry to the corresponding decay amplitude $H \rightarrow q\bar{q}q\bar{q}$. The QCD and EW NLO corrections to these decays were discussed in detail in Refs. [18,19]; in particular, a representative set of Feynman diagrams can be found there.

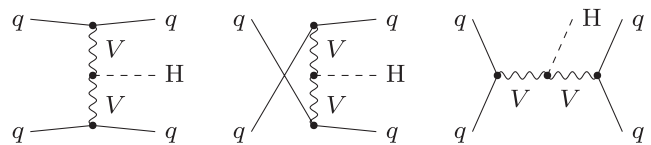


FIG. 1. Topologies for t -, u -, and s -channel contributions to $qq \rightarrow qqH$ in LO, where q denotes any quark or antiquark and V stands for W and Z bosons.

Evaluating $2 \rightarrow 3$ particle processes at the NLO level is nontrivial, both in the analytical and numerical parts of the calculation. In order to ensure the correctness of our results we have evaluated each ingredient twice, resulting in two completely independent computer codes yielding results in mutual agreement. The phase-space integration is performed using multichannel Monte Carlo techniques [20] implemented in different ways in the two different generators.

Virtual corrections.—The virtual corrections modify the partonic processes that are already present at LO; there are about 200 EW one-loop diagrams per tree diagram in each flavor channel. At NLO these corrections are induced by self-energy, vertex, box (4-point), and pentagon (5-point) diagrams. The calculation of the one-loop diagrams has been performed in the conventional 't Hooft–Feynman gauge and in the background-field formalism using the conventions of Refs. [21,22], respectively. The masses of the external fermions have been neglected whenever possible, i.e., everywhere but in the mass-singular logarithms.

In the s -channel diagrams intermediate W and Z bosons can become resonant, corresponding to WH/ZH production with subsequent gauge-boson decay. In order to consistently include these resonances, we implement the finite widths of the gauge bosons in the “complex-mass scheme,” which was introduced in Ref. [23] for LO calculations and generalized to the one-loop level in Ref. [24]. In this approach the W - and Z -boson masses are consistently considered as complex quantities, defined as the locations of the propagator poles in the complex plane. The scheme fully respects all relations that follow from gauge invariance.

The amplitudes have been generated with FEYNARTS, using the two independent versions 1 [25] and 3 [26]. The algebraic evaluation has been performed in two completely independent ways. One calculation is based on the in-house MATHEMATICA program that was already used in the algebraic reduction of NLO corrections to the $H \rightarrow 4$ fermions decays [18,19]. The other has been completed with the help of FORMCALC [27].

The tensor integrals are evaluated as in the calculation of the corrections to $e^+e^- \rightarrow 4$ fermions [24,28]. They are recursively reduced to master integrals at the numerical level. The scalar master integrals are evaluated for complex masses using the methods and results of Refs. [29–31]. Tensor and scalar 5-point functions are directly expressed in terms of 4-point integrals [32]. Tensor 4-point and 3-point integrals are reduced to scalar integrals with the Passarino-Veltman algorithm [33] as long as no small Gram determinant appears in the reduction. If small Gram determinants occur, the alternative schemes described in Ref. [34] are applied.

Real corrections.—Real QCD corrections consist of gluon emission and processes with gq and $g\bar{q}$ initial states. Analogously real photonic corrections comprise photon bremsstrahlung and photon-induced processes with γq and $\gamma\bar{q}$ initial states. The matrix elements for these

corrections have been evaluated using the Weyl–van der Waerden spinor technique as formulated in Ref. [35] and have been checked against results obtained with MADGRAPH [36].

All types of real corrections involve singularities from collinear initial-state splittings which are regularized with small quark masses. The mass singularities are absorbed via factorization by the usual PDF redefinition both for the QCD and photonic corrections (see, e.g., Ref. [37]). Technically, the soft and collinear singularities for real gluon or photon emission are isolated both in the dipole subtraction method following Ref. [38] and in the phase-space slicing method. For gluons or photons in the initial state the subtraction and slicing variants described in Ref. [37] are applied. The results presented in the following are obtained with the subtraction method, which numerically performs better.

Numerical results.—We use the input parameters as given in Ref. [18]. Since quark-mixing effects are suppressed, we set the Cabibbo–Kobayashi–Maskawa matrix to the unit matrix. The electromagnetic coupling is fixed in the G_μ scheme; i.e., it is set to $\alpha_{G_\mu} = \sqrt{2}G_\mu M_W^2 s_w^2 / \pi$, because this accounts for electromagnetic running effects and some universal corrections of the ρ parameter.

We use the MRST2004QED PDF [39], which consistently include $\mathcal{O}(\alpha)$ QED corrections. These PDF include a photon distribution function for the proton and thus allow to take into account photon-induced partonic processes. As explained in Ref. [37], to consistently use these PDF one must calculate the QCD corrections using the $\overline{\text{MS}}$ factorization scheme and the QED corrections using the DIS scheme; the corresponding factorization scales are identified with the Higgs boson mass M_H if not stated otherwise. We only use four quark flavors for the initial partons; i.e., we do not take into account the contribution of bottom quarks, which is suppressed. Since no associated LO version of the MRST2004QED PDF exists, we use these PDF both for LO and NLO predictions. For the renormalization scale of the strong coupling constant by default we employ M_H , include 5 flavors in the two-loop running, and fix $\alpha_s(M_Z) = 0.1187$.

Apart from the total cross section without any phase-space cuts, we consider the integrated cross section defined after applying typical VBF cuts to the outgoing jets. In this case, jets are defined from partons using the k_T algorithm [40–42] as described in Ref. [43]. More precisely, jets result from partons of pseudorapidity $|\eta| < 5$ using the jet resolution parameter $D = 0.8$. We also recombine real photons with partons or jets according to this algorithm. Thus, some of the photons end up in jets; others are left as identifiable photons. Following Ref. [16], we specify the VBF cuts as follows. We require at least two hard jets with

$$p_{Tj} \geq 20 \text{ GeV}, \quad |y_j| \leq 4.5, \quad (1)$$

where p_{Tj} is the transverse momentum of the jet and y_j its rapidity. The tagging jets j_1 and j_2 are then defined as the

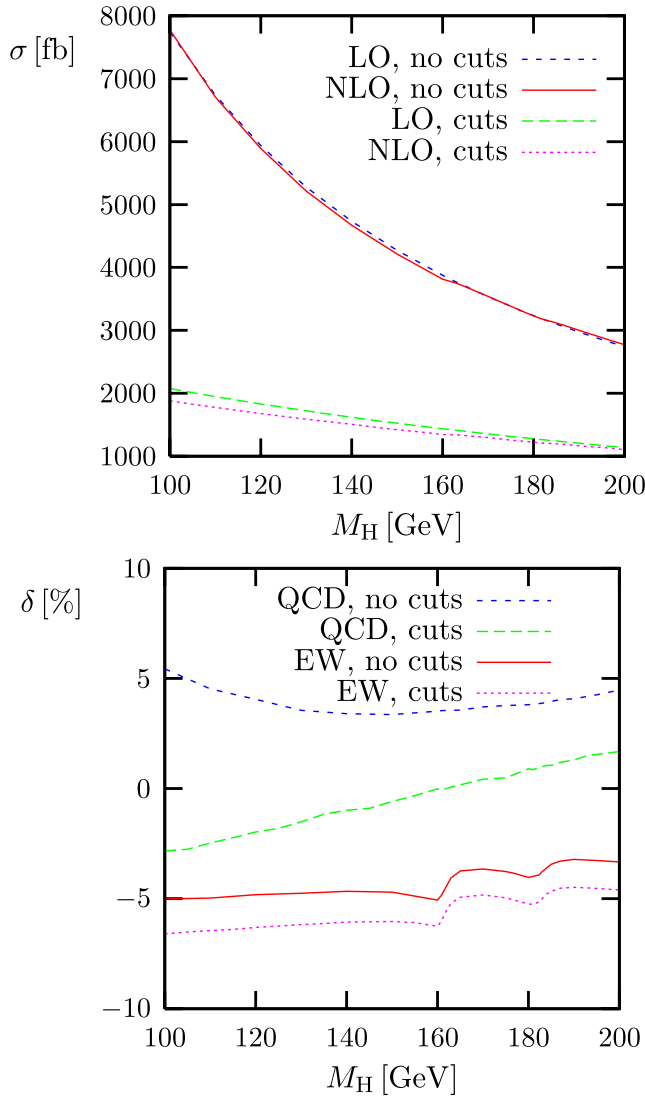


FIG. 2 (color online). Higgs boson mass dependence of LO and complete NLO cross section (upper) and relative EW and QCD corrections (lower) without and with VBF cuts.

two jets passing the cuts (1) with highest p_T and $p_{Tj_1} > p_{Tj_2}$. Finally, we demand a large rapidity separation of the two tagging jets by

$$\Delta y_{jj} \equiv |y_{j_1} - y_{j_2}| > 4, \quad y_{j_1} y_{j_2} < 0. \quad (2)$$

In Fig. 2 we plot the total cross section with and without cuts as a function of M_H . In the upper panel we show the absolute predictions in LO and in NLO including QCD and EW corrections. The VBF cuts reduce the cross section by a factor 3–4. In the lower panel we show the relative corrections. Without cuts the QCD corrections are about +5% and the EW corrections about –5%, both depending only weakly on M_H and canceling each other substantially. With cuts the EW corrections are approximately –6%, while the QCD corrections vary between –3% and +2%. In the EW corrections the WW and ZZ thresholds are clearly visible. It is interesting to note that the EW

TABLE I. Cross section for $pp \rightarrow H + 2 \text{ jets} + X$ in LO and NLO without cuts and relative QCD and EW corrections. The contribution $\delta_{\gamma\text{-induced}}$ from γ -induced processes (which is part of δ_{EW}) is also given separately.

| M_H [GeV] | 120 | 150 | 170 | 200 |
|--------------------------------------|----------|----------|----------|----------|
| σ_{LO} [fb] | 5936(1) | 4271(2) | 3536(1) | 2743(1) |
| σ_{NLO} [fb] | 5890(2) | 4219(2) | 3538(1) | 2775(1) |
| δ_{QCD} [%] | 4.04(3) | 3.47(2) | 3.72(2) | 4.48(2) |
| δ_{EW} [%] | –4.81(2) | –4.70(2) | –3.65(1) | –3.33(1) |
| $\delta_{\gamma\text{-induced}}$ [%] | 0.86(1) | 1.04(1) | 1.14(1) | 1.27(1) |

corrections to the full VBF channel are similar in size and sign to the EW corrections to the subreactions $pp \rightarrow WH/ZH + X$ [44]. Compared to the related decays $H \rightarrow WW/ZZ \rightarrow 4f$ [18,19] the size is similar, but the sign is different.

In Table I we present integrated cross sections for $M_H = 120, 150, 170,$ and 200 GeV without any cuts and in Table II results for VBF cuts. We list the LO cross section σ_{LO} , the cross section σ_{NLO} including QCD + EW corrections, and the relative QCD and EW corrections, δ_{QCD} and δ_{EW} , respectively. The complete EW corrections δ_{EW} also comprise the corrections from photon-induced processes $\delta_{\gamma\text{-induced}}$, which turn out to be $\sim +1\%$ and to reduce the EW corrections.

In Fig. 3 we show the dependence of the total cross section on the factorization and renormalization scale for $M_H = 120$ GeV. We set the factorization scale $\mu \equiv \mu_F$, which applies to both QCD and QED contributions, equal to the renormalization scale $\mu_R = \mu$ and vary it between $M_H/8$ and $8M_H$. In this setup, we show the LO cross section, the QCD corrected NLO cross section and the complete NLO cross section involving both QCD and EW corrections. In addition we depict the QCD corrected NLO cross section for the setup where $\mu_R = M_H^2/\mu$ (NLO QCD'). Varying the scale μ up and down by a factor 2 (8) changes the cross section by 11% (29%) in LO and 3% (18%) in NLO for the setup with VBF cuts.

Conclusions.—Radiative corrections of strong and electroweak interactions have been discussed at next-to-leading order for Higgs boson production via vector-boson fusion at the LHC. The electroweak corrections, which have not been calculated before, reduce the cross section by 5% and are thus as important as the QCD corrections in this channel.

TABLE II. As in Table I, but with VBF cuts applied.

| M_H [GeV] | 120 | 150 | 170 | 200 |
|--------------------------------------|-----------|-----------|-----------|-----------|
| σ_{LO} [fb] | 1830.5(5) | 1524.2(4) | 1353.8(3) | 1139.1(3) |
| σ_{NLO} [fb] | 1678.7(9) | 1422.9(7) | 1293.4(6) | 1106.0(5) |
| δ_{QCD} [%] | –1.97(4) | –0.60(4) | 0.41(4) | 1.76(3) |
| δ_{EW} [%] | –6.32(2) | –6.02(2) | –4.87(1) | –4.64(1) |
| $\delta_{\gamma\text{-induced}}$ [%] | 1.14(1) | 1.21(1) | 1.25(1) | 1.31(1) |

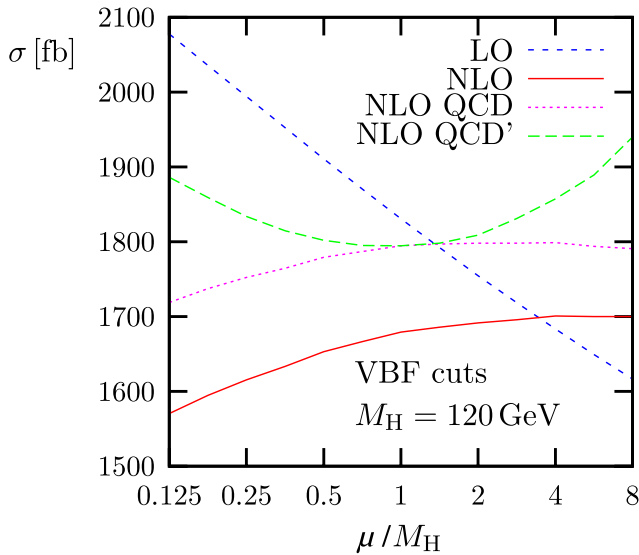


FIG. 3 (color online). Scale dependence of LO and NLO cross sections with QCD or QCD + EW corrections for $M_H = 120$ GeV with VBF cuts, $\mu_R = \mu_F \equiv \mu$ for LO, NLO, and NLO QCD, but $\mu_R = M_H^2/\mu$ for NLO QCD'.

This work is supported in part by the European Community's Marie Curie Research Training Network HEPTOOLS under Contract No. MRTN-CT-2006-035505. We thank M. Spira for comments on the manuscript.

-
- [1] S. Asai *et al.*, Eur. Phys. J. C **32S2**, s19 (2004).
 [2] S. Abdullin *et al.*, Eur. Phys. J. C **39S2**, s41 (2005).
 [3] J. Alcaraz *et al.* (ALEPH), arXiv:hep-ex/0612034.
 [4] V. Del Duca *et al.*, J. High Energy Phys. 10 (2006) 016.
 [5] V.D. Barger, R.J.N. Phillips, and D. Zeppenfeld, Phys. Lett. B **346**, 106 (1995).
 [6] D.L. Rainwater and D. Zeppenfeld, J. High Energy Phys. 12 (1997) 005.
 [7] D.L. Rainwater, D. Zeppenfeld, and K. Hagiwara, Phys. Rev. D **59**, 014037 (1999).
 [8] D.L. Rainwater and D. Zeppenfeld, Phys. Rev. D **60**, 113004 (1999).
 [9] A. Djouadi, arXiv:hep-ph/0503172.
 [10] M. Spira, Fortschr. Phys. **46**, 203 (1998).
 [11] V. Del Duca *et al.*, Nucl. Phys. B **616**, 367 (2001).
 [12] J.M. Campbell, R. Keith Ellis, and G. Zanderighi, J. High Energy Phys. 10 (2006) 028.
 [13] M.V. Acosta and A. Nikitenko, arXiv:0705.3585.
 [14] T. Han, G. Valencia, and S. Willenbrock, Phys. Rev. Lett. **69**, 3274 (1992).
 [15] T. Figy, C. Oleari, and D. Zeppenfeld, Phys. Rev. D **68**, 073005 (2003).
 [16] T. Figy and D. Zeppenfeld, Phys. Lett. B **591**, 297 (2004).
 [17] E.L. Berger and J. Campbell, Phys. Rev. D **70**, 073011 (2004).
 [18] A. Bredenstein, A. Denner, S. Dittmaier, and M.M. Weber, Phys. Rev. D **74**, 013004 (2006).
 [19] A. Bredenstein, A. Denner, S. Dittmaier, and M.M. Weber, J. High Energy Phys. 02 (2007) 080.
 [20] J. Hilgart, R. Kleiss, and F. Le Diberder, Comput. Phys. Commun. **75**, 191 (1993).
 [21] A. Denner, Fortschr. Phys. **41**, 307 (1993).
 [22] A. Denner, S. Dittmaier, and G. Weiglein, Nucl. Phys. B **440**, 95 (1995).
 [23] A. Denner, S. Dittmaier, M. Roth, and D. Wackerroth, Nucl. Phys. B **560**, 33 (1999).
 [24] A. Denner, S. Dittmaier, M. Roth, and L.H. Wieders, Nucl. Phys. B **724**, 247 (2005).
 [25] J. Küblbeck, M. Böhm, and A. Denner, Comput. Phys. Commun. **60**, 165 (1990).
 [26] T. Hahn, Comput. Phys. Commun. **140**, 418 (2001).
 [27] T. Hahn and M. Pérez-Victoria, Comput. Phys. Commun. **118**, 153 (1999).
 [28] A. Denner, S. Dittmaier, M. Roth, and L.H. Wieders, Phys. Lett. B **612**, 223 (2005).
 [29] A. Denner, U. Nierste, and R. Scharf, Nucl. Phys. B **367**, 637 (1991).
 [30] G. 't Hooft and M.J.G. Veltman, Nucl. Phys. B **153**, 365 (1979).
 [31] W. Beenakker and A. Denner, Nucl. Phys. B **338**, 349 (1990).
 [32] A. Denner and S. Dittmaier, Nucl. Phys. B **658**, 175 (2003).
 [33] G. Passarino and M.J.G. Veltman, Nucl. Phys. B **160**, 151 (1979).
 [34] A. Denner and S. Dittmaier, Nucl. Phys. B **734**, 62 (2006).
 [35] S. Dittmaier, Phys. Rev. D **59**, 016007 (1999).
 [36] T. Stelzer and W. Long, Comput. Phys. Commun. **81**, 357 (1994).
 [37] K.P.O. Diener, S. Dittmaier, and W. Hollik, Phys. Rev. D **72**, 093002 (2005).
 [38] S. Dittmaier, Nucl. Phys. B **565**, 69 (2000).
 [39] A.D. Martin, R.G. Roberts, W.J. Stirling, and R.S. Thorne, Eur. Phys. J. C **39**, 155 (2005).
 [40] S. Catani, Y.L. Dokshitzer, and B.R. Webber, Phys. Lett. B **285**, 291 (1992).
 [41] S. Catani, Y.L. Dokshitzer, M.H. Seymour, and B.R. Webber, Nucl. Phys. B **406**, 187 (1993).
 [42] S.D. Ellis and D.E. Soper, Phys. Rev. D **48**, 3160 (1993).
 [43] G.C. Blazey *et al.*, arXiv:hep-ex/0005012.
 [44] M.L. Ciccolini, S. Dittmaier, and M. Krämer, Phys. Rev. D **68**, 073003 (2003).